

Article

Investigation of Energy-Efficient Solutions for a Single-Family House Based on the 4E Idea in Poland

Piotr Ciuman ¹, Jan Kaczmarczyk ^{1,*}  and Dorota Winnicka-Jasłowska ² 

¹ Department of Heating, Ventilation and Dust Removal Technology, Faculty of Energy and Environmental Engineering, Silesian University of Technology, ul. Konarskiego 18, 44-100 Gliwice, Poland; piotr.ciuman@polsl.pl

² Department of Design and Architectural Research, Faculty of Architecture, Silesian University of Technology, ul. Akademicka 7, 44-100 Gliwice, Poland; dorota.winnicka-jaslowska@polsl.pl

* Correspondence: jan.kaczmarczyk@polsl.pl; Tel.: +48-323272820

Abstract: The paper analyses multi-variant energy simulations carried out in IDA ICE 4.8 software for a newly designed single-family building within the framework of the 4E Idea. This idea assumes the use of energy-saving, ecological, ergonomic, and economic solutions in construction and building operation. Energy simulations were conducted to evaluate the annual energy-saving potential of the developed architectural house concept, which incorporates ergonomic analyses and cost-effective construction solutions. Analyses were conducted to optimise the non-renewable primary energy index by selecting mechanical ventilation system (CAV or VAV) with heat recovery; the configuration of photovoltaic module installation in terms of their location and orientation; the exposure and type of solar thermal collectors (flat and vacuum); and the use of two types of heat pumps (air- and ground-source). The most favourable energy performance of the building was achieved with an HVAC system equipped with a VAV mechanical ventilation system with heat recovery, an on-grid photovoltaic installation, vacuum solar thermal collectors, and a ground-source heat pump with a horizontal heat exchanger. This configuration resulted in a primary energy index value of 2 kWh/m²/year. The results of the analyses carried out for the 4E building concept may serve as a reference point for future energy-efficient building designs aspiring to meet higher standards of sustainable development.

Keywords: renewable energy sources; energy performance; single-family building; heat pump; solar thermal collector; photovoltaics; energy analyses



Academic Editor: Konstantinos E. Kounetas

Received: 11 December 2024

Revised: 7 January 2025

Accepted: 12 January 2025

Published: 20 January 2025

Citation: Ciuman, P.; Kaczmarczyk, J.; Winnicka-Jasłowska, D. Investigation of Energy-Efficient Solutions for a Single-Family House Based on the 4E Idea in Poland. *Energies* **2025**, *18*, 449. <https://doi.org/10.3390/en18020449>

Copyright: © 2025 by the authors. Licensee MDPI, Basel, Switzerland. This article is an open access article distributed under the terms and conditions of the Creative Commons Attribution (CC BY) license (<https://creativecommons.org/licenses/by/4.0/>).

1. Introduction

The global goal of reducing energy consumption in buildings and mitigating their environmental impact continues to challenge the architectural, engineering and construction sectors. Maintaining high-quality comfort in terms of building functionality and occupant satisfaction is an additional challenge and, therefore, requires the application of a person-centred design of physical and social environments [1]. These challenges apply to all types of buildings, but due to the prolonged time people spend indoors, residential buildings are particularly important.

In Poland, single-family buildings accounted for 97.5% of all new residential buildings constructed in the first quarter of 2024. Almost all of these buildings, i.e., 98.2%, were constructed using traditional, improved technologies [2].

Statistical data show that over many years the household sector in the European Union has consistently contributed significantly to the final energy consumption [3]. In

2021, households made up a large proportion of the national energy consumption in EU countries, ranging from 11.4% (Luxembourg) to 28.1% (Croatia). In Poland, this indicator was 20.2% and was higher than the EU average (18.4%) [4]. In recent years, residential buildings in Poland have consumed the most energy: approximately 66% for space heating, followed by domestic hot water preparation (17%), lighting and electrical applications (9%), and cooking (8%) [5].

The building sector in the EU is also a substantial contributor to greenhouse gas emissions in the EU. In 2022, it was responsible for 34% of energy-related emissions [6]. Analyses of the whole life cycle performed for a single-family house showed that the greatest contributor to the environmental effects was the energy consumed during building operation, which contributed to 58% to 90% of the CO₂ emissions [7]. Heating-related energy consumption is one of the main sources of greenhouse gas emissions and accounts for a large part of domestic energy use. Reducing heating-related energy consumption offers great potential to reduce Europe's greenhouse gas emissions. The analysis also showed that facilities using heat pumps are characterised by an environmental impact that is six times lower than that of facilities powered by coal combustion and electricity from the network. Similarly, the social costs associated with CO₂ emissions were significantly lower in the case of the use of renewable energy sources [7]. It should be noted that in Poland, despite the increased share of renewable sources in electricity production, hard coal still has a significant share. In 2023, hard coal accounted for just over 60% of total energy generation, while renewable energy sources contributed approximately 25% (wind 14%, photovoltaics (PV) solar 6.8%, and biofuels 4.7%) [8].

In the single-family home sector, a viable option is the production of electricity by photovoltaic modules and its efficient on-site use. Thus, the application of PV panels with heat pumps [9–11] and domestic hot water systems [12] is a promising solution. Several studies have proven that such a combination can increase monthly self-consumption from 7% to 18%, and annually up to 13% [13]. An advanced smart-grid-ready controlled PV-HP-battery system in a single-family household showed that, over one-year operation, self-consumption can be increased even further, up to 43% [14]. The performance evaluation of a combination of heat pump and PV system controlled by a novel algorithm and based on simulations showed that between 25.3% and 41.0% of the building's electricity consumption, including the heat pump, can be covered directly by the PV installation annually. It was noted that the characteristics of the heating system can significantly influence the results. New buildings with floor heating and low supply temperatures yield a higher PV self-consumption levels compared to buildings with radiator heating and higher supply temperatures. The addition of a battery to the system further increased the degree of PV self-consumption. It was also noted that due to the high investment costs of batteries, they do not pay off within a reasonable period [12]. Another study in a Danish single-family house with a heat pump and floor heating [15], experimentally demonstrated that load shifting may be feasible and cost-effective, even without energy storage, and that the current pricing scheme, which allows the grid operators to differentiate the end-user tariffs throughout the day, provides a stimulus for end-consumers to shift heating loads. In addition, it has been shown that space heating systems in Swedish houses equipped with heat pumps have the potential to increase the resilience of the power grid during major network disruptions by temporarily reducing the room temperature to an acceptable level for the users [16].

Energy used in a building, apart from heating and hot water production [17], is to a large extent intended for heating (or cooling) the ventilation air. In accordance with the requirements in Poland, the supply air volume flow rate in residential premises should be constant and should correspond to the exhaust air volume flow rate planned for the

ventilation of kitchens and bathrooms. However, it should not be less than 20 m³/h per person intended for permanent residence in the building design [18]. The installation of a Variable Air Volume (VAV) system working with the demand–control principle can noticeably reduce source energy and energy costs. Study measurements were carried out in a 140 m² single-family house occupied by two adults and two children, where the controls installed in the existing mechanical ventilation system showed that the ventilation operation can be reduced to a low rate of running 37% of the time without significant changes in the CO₂ concentration and moisture level in the house. Savings in electrical energy for running fans were estimated at 35% [19]. Another study suggested that the VAV system can be especially beneficial to houses in cooling-dominant climates [20]. In Poland, due to legal restrictions, the VAV solution is not used, but its effectiveness is worth investigating, especially if the air quality is not compromised.

Reduction in the amount of energy for ventilation air treatment can be achieved by using appropriate heat recovery solutions and their frost control [21] or application of a ground heat exchanger [22]. The operation of the ventilation system is essential for removing air pollutants generated in the room and to maintain appropriate indoor air quality. In residential buildings the primary pollutants are those related to occupants and their activity, mainly bioeffluents represented by CO₂ and humidity. Other indoor sources are building materials and equipment emitting VOCs [23], which is especially important in newly built houses. The pollution emission rate is strongly influenced by the occupancy patterns [24]. The emission from building materials is continuous, although it is strongest for new materials and decreases in time. One option to reduce emissions from the building is the use of green materials [25]. However, it is necessary to provide measures to mitigate risks and to remove the pollution. Studies performed in 25 energy-efficient residential buildings with mechanical ventilation showed lower concentrations of indoor PM10, PM2.5, CO₂, and VOCs compared to conventional apartments. Also, the prevalence of symptoms, particularly children’s atopic dermatitis and allergic rhinitis, was significantly lower. Occupants showed a higher satisfaction level with their sleep quality, indoor air, and indoor humidity than in conventional apartments [26].

Addressing these challenges requires innovative design strategies and technologies that balance energy efficiency, environmental protection, economic viability, and user comfort—the cornerstones of the 4E Idea [27]. The main assumptions of the 4E Idea model single-family house project were:

- Energy saving;
- Ecology, including: management of rainwater and limiting its collection from the network, use of construction materials from recycling to the greatest extent possible and with the lowest possible carbon footprint;
- Economy, low investment and operational costs over the life cycle;
- Ergonomics, design solutions based on the analysis of the real needs of users in different age groups, a building designed based on the principles of ergonomics.

The second assumption of the project was IDEA 2+2+(1), which assumes surface and functional–spatial solutions for a family with a changing number of members at different stages of the building’s life, i.e., two, four, or five family members. The project assumed space flexibility, which can easily be rearranged or expanded. For this purpose, pre-designed studies were carried out, which allowed for the definition of the guidelines for the project.

The topic of energy-efficient and environmentally friendly buildings, along with the search for appropriate technical solutions, has been the focus of numerous studies in recent years [28]. Most of these studies address individual aspects, such as the use of photovoltaic panels or the optimisation of heat pump performance. However, only a few studies consider

multiple factors simultaneously. A novelty of the study presented in this manuscript lies in the comprehensive consideration of the building as a whole, including its construction and technical systems. The primary goal was to identify a combination of solutions that would enable a single-family house to achieve zero-energy status.

This paper focuses primarily on the problems of energy production and consumption and indicates solutions that include renewable energy sources and advanced HVAC systems, which will allow the goal of creating a zero-energy 4E Idea building to be achieved. In addition to demonstrating the impact of the type of PV installation, solar thermal collectors, and the type of heat pump, which was the subject of previous studies, the presented analyses also raised the issue of the justification for using a CO₂ concentration-controlled VAV mechanical ventilation system to reduce energy consumption and the non-renewable primary energy index. The analyses were conducted based on energy simulations of the building designed for the local climate of Poland. The calculations used the IDA ICE simulation tool, which has been previously used in many energy analyses of buildings, including analyses of the operation of renewable energy sources [12,29–31]. Although IDA ICE does not take into account the directionality effects of direct solar radiation [32], it has been proven to accurately predict building thermal behaviour [33,34]. As a result of the activities carried out, a concept of an energy-efficient building was developed, which in terms of architecture, construction, and the configuration of the HVAC system and renewable energy sources can be a starting point for future projects of energy-efficient single-family buildings. It can also contribute to the development of energy-efficient single-family homes that align with Poland's environmental goals and global sustainability standards.

2. Materials and Methods

2.1. Characteristics of the Designed Building and Assumptions for the Simulation

The analysed facility was a newly designed single-family building that is detached, single-storey, without a basement, and consisting of two cuboid-shaped parts covered with gable roofs intersecting in the central part of the building. The building was divided into four zones: the entrance zone—connecting the daytime and nighttime zones, as well as the garage and utility rooms; the daytime zone—an open space comprising the living room, kitchen, and access to the terrace; the nighttime zone—a private area containing bedrooms and a bathroom; and the utility zone. A non-habitable attic was located above the nighttime and utility zones. The usable floor area of the building was 147 m². Including the garage, the total area was 189.7 m², with a total volume of 583 m³. Typically, the area of a house for a family of four in Poland is approximately 120–150 m², with an average of 132.6 m² [2]. This space typically includes two rooms for the children, a bedroom for the parents, a shared living room, a kitchen, a bathroom, a toilet, and an additional room.

The 1300 m² plot was initially divided into four zones: the northern zone, designated for entrance and utility functions; the eastern and south-eastern zone, allocated for the installation of a ground heat exchanger; and the southern, south-western, and western zones, intended for leisure and recreational purposes, which together constituted the largest part of the plot.

The daytime zone of the building, characterised by the largest glazed area on the external wall, was oriented southward to maximise solar heat gains and thereby reduce the building's energy consumption. Figure 1 presents the building's floor plan, showing the division into daytime and nighttime zones, along with the detailed layout and floor areas of the rooms. Figure 2 shows the visualisation of the building's southern façade and the interior of the living room with the kitchen.

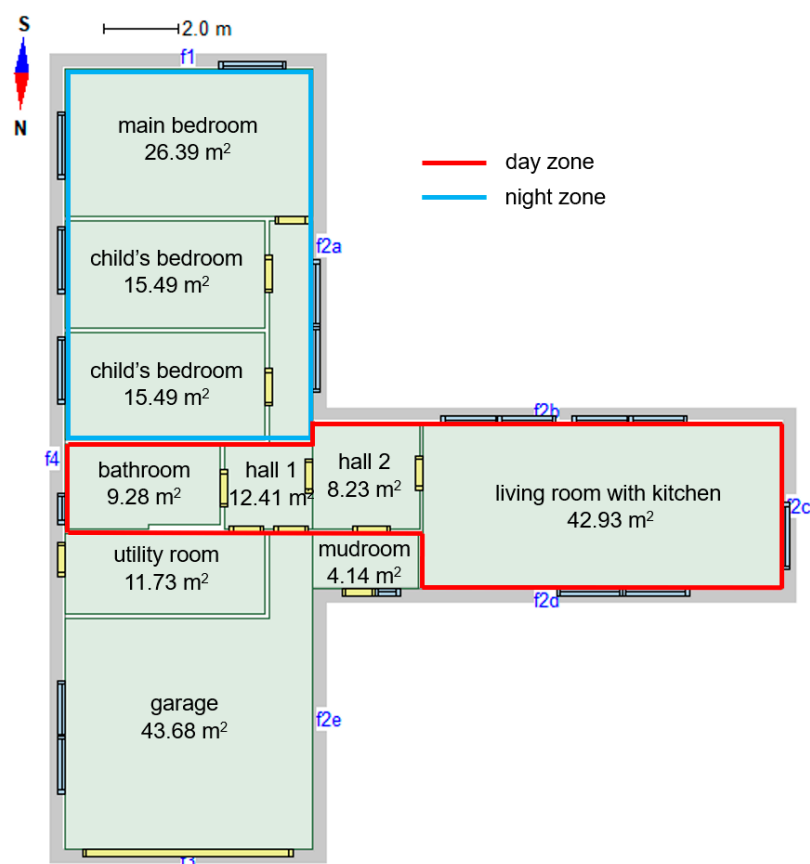


Figure 1. Floor plan of the designed building, created using IDA ICE 4.8 software.



(a)



(b)

Figure 2. Visualisation of the building's southern façade (a) and interior of the living room with the kitchen (b).

The height of the rooms in the nighttime (private) zone was 2.95 m, while in the daytime (functional) zone, the height at the peak line of the roof was 4.90 m. The largest room in the daytime part of the building was the living room with the kitchen. This part of the building featured a gable roof, with exposed trusses inside, as well as large windows on the southern side. The glazing area accounted for 53% of the surface area of the southern external wall. The nighttime zone contained two children's bedrooms, the main (larger) master bedroom, and a bathroom. Additionally, the building included a garage with parking space for two cars and a utility room, which housed the domestic hot water storage tank, a heat recovery ventilation unit (HRV), and other HVAC and electrical system equipment. The connecting space between the two parts of the building was a corridor with large windows opening onto the terrace. In all rooms, except for the non-habitable

attic, the air temperature was adjustable. Figures 3 and 4 depict the façades and a 3D view of the geometric model of the building, created using the IDA ICE 4.8 software.



Figure 3. Views of the designed building's façades—(a) northern façade, (b) eastern façade, (c) southern façade, created using IDA ICE 4.8 software.

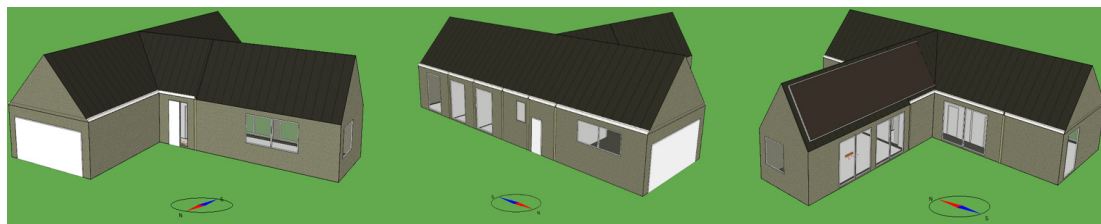


Figure 4. Three-dimensional views of the designed building, created using IDA ICE 4.8 software.

The building structure consisted of an external and internal arrangement of load-bearing brick walls supported on a foundation slab, which incorporated a heating system installation and was covered by a trussed roof.

The heat transfer coefficient of individual building partitions was calculated based on the type and thickness of the construction materials comprising these partitions. The proper materials were preselected based on their thermal properties and costs. The partitions were designed to ensure that their heat transfer coefficient did not exceed the maximum value specified in the standard [34]. Table 1 presents their structure and heat transfer coefficients.

The building was designed with a heating, ventilation, and air conditioning (HVAC) system equipped with renewable energy sources. The heating system consisted of heating elements in the form of floor heating with operating parameters of 35 °C/30 °C. These parameters are widely used due to their compatibility with low-temperature heating sources, such as heat pumps. They are commonly recommended in industry guidelines and standards for residential heating systems of well-insulated buildings. In the garage, a wall-mounted panel radiator was installed.

The heat source for the heating and domestic hot water systems was an air-source heat pump with a nominal heating capacity of 6.1 kW and a coefficient of performance (COP) of 5.2 (for an air inlet temperature of 7 °C and a hot water temperature at the heat pump outlet of 35 °C). The system was supplemented with a buffer tank. The heating power of the radiators and the heat pump was selected based on the calculated heat demand of the building and individual rooms. The heating system was equipped with an automatic air temperature regulation system for rooms, based on the set minimum air temperature values: 24 °C for bathrooms, 20 °C for rooms designated for regular occupancy, 16 °C for the utility room, and 8 °C for the garage [35]. The domestic hot water system was designed with a 300-litre storage tank. In heating mode, the heat pump was activated when indoor air temperature fell below the heating setpoint. Heat was transferred to the buffer tank, which supplied energy to the space heating system. The heat pump prioritised domestic hot water production when the hot water tank temperature dropped below a specific setpoint (55 °C). The system switched to domestic hot water mode when hot water demand was detected, with priority over space heating to ensure uninterrupted hot water supply. The heat pump operated at optimal efficiency by modulating its output based on

outdoor air temperature and load requirements. During mild weather, the heat pump ran at lower capacity, while at peak demand, it operated at full capacity.

Table 1. Construction of external building partitions and their heat transfer coefficients. The layers are presented in order from the inner side to the outer side of the building.

Building Partition	Construction	Heat Transfer Coefficient U , W/m ² K
External wall	<ul style="list-style-type: none"> - cement–lime plaster - brick wall made of perlite blocks in SYSTEM 3E, 35.2 cm thick - mineral wool (insulation), 8 cm thick - cement–lime plaster 	0.14
Roof	<ul style="list-style-type: none"> - plasterboard - vapour barrier foil - polyurethane foam PUR/PIR - mineral wool, 36 cm thick - pine wood class C27 - roofing membrane - flat roof tile Actua 10 	0.08
Ground floor slab	<ul style="list-style-type: none"> - glass tiles - primer, 6 cm thick - damp proofing - reinforced concrete slabs, 50 cm thick - XPS Styrofoam, 20 cm thick - substrate made of gravel, gravel and coarse sand, 50 cm thick 	0.14
Ceiling under the unheated attic	<ul style="list-style-type: none"> - cement–lime plaster - SMART type compressed plates, 15 cm thick - mineral wool, 30 cm thick 	0.11
Windows		0.9
External door		1.3

The mechanical supply and exhaust ventilation system was equipped with a cross-flow heat recovery unit (HRV) with an efficiency of 80%, along with an air heater with a glycol heat exchanger and a ground heat exchanger (GHE) that helps save electricity by cooling the supply air in the summer while pre-heating it in the winter. The type of mechanical ventilation system, with variable air volume (VAV) or constant air volume (CAV) flow rates, was selected based on the analysis results presented in Section 3. The cross-flow heat exchanger in the HRV recovered heat from exhaust air to preheat incoming fresh air during cold seasons. In the summer, the heat recovery function operated in reverse to avoid overheating the incoming air. The air heater (connected to the horizontal GHE) was used to condition the supply air further when the preheated air did not meet the desired temperature. The heater was activated based on real-time indoor air temperature and demand. The GHE preconditioned incoming fresh air by exchanging heat with the ground. In the winter, it preheated cold outdoor air to reduce the load on the ventilation system and the air heater. In the summer, it cooled the warm outdoor air, providing passive cooling and reducing the need for active cooling systems.

The building was also planned to be equipped with an on-grid photovoltaic system aimed at covering the building's electricity demand, including the operation of HVAC components, such as the heat pump. A self-consumption rate of 40% of the produced electricity was assumed [36,37]. The location of the photovoltaic modules was also de-

terminated based on the results of the analysis presented in Section 3. In IDA ICE, the energy generated by the PV system depends on solar radiation data from a weather file. This file contains hourly values for global and diffuse solar radiation, which is essential for simulating localised energy output. Users can select or define a specific weather file, enabling real-time calculations based on solar radiation, panel efficiency, environmental conditions, and system losses.

Additionally, two rainwater collection tanks were planned on the plot around the building to support the toilet flushing system and the garden irrigation system.

Figure 5 shows the schematic diagram of the designed HVAC and photovoltaic systems within the building.

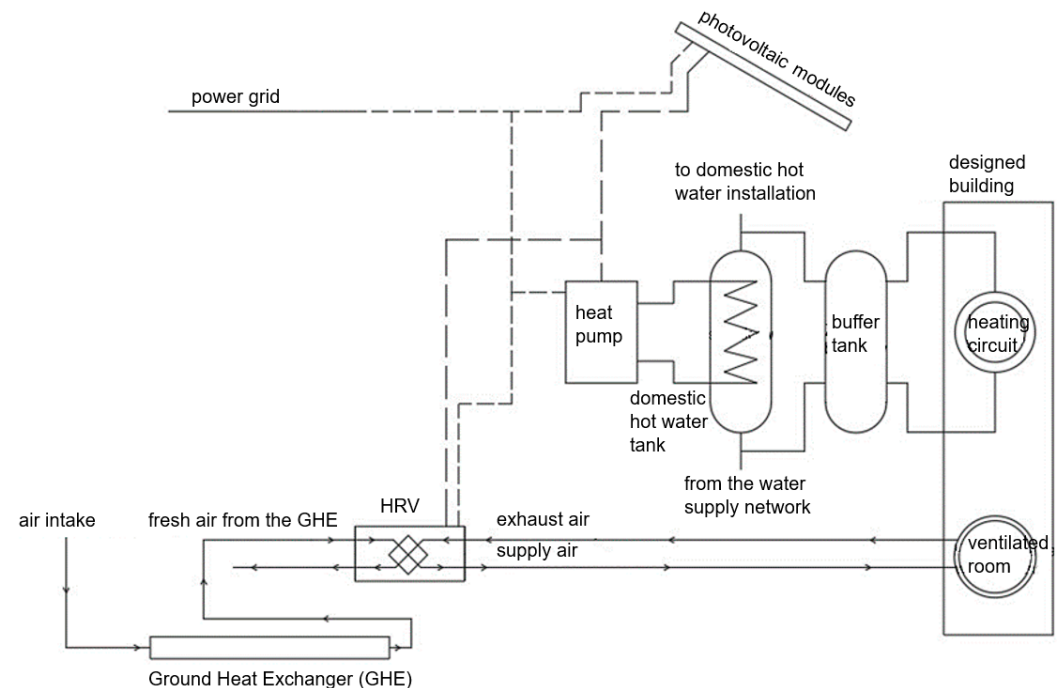


Figure 5. Schematic diagram of the HVAC and photovoltaic installation in the designed building.

2.2. Research Methodology

Year-round energy demand analyses for various computational variants were carried out using the IDA ICE 4.8 software [38]. This is an advanced software tool for conducting energy simulations and thermal comfort analysis in buildings. It is used by designers, engineers, and architects to assess the energy efficiency of buildings and ensure optimal thermal comfort for occupants. The software allows for detailed building modelling, considering the geometric and material properties of the building as well as the parameters of the HVAC system. With the ability to simulate various climatic conditions, IDA ICE enables the evaluation of the impact of year-round climatic conditions on energy consumption and occupants' comfort in buildings.

A geometric model of the designed building defining the construction of the building's envelope and elements, and orienting it according to the cardinal directions, was created in the IDA ICE 4.8 software in line with the design assumptions. The building was located in Katowice, Poland, for which climatic data from the ASHRAE database [39] were available. Default values for thermal bridges were assumed. The minimum outdoor air exchange rate was set to 0.5 L/h [35]. The numerical model included heat gains from occupants, electronic equipment, and lighting. It was assumed that the building would house four people: two adults and two children. For each zone (room), an occupancy schedule was set depending on the room's intended use. In bedrooms, occupants were assumed to be present during

nighttime hours (22:00–06:00), while in the daytime zones, higher occupancy was assumed during the afternoon and evening hours (15:00–20:00), reflecting typical household routines after returning home from work or school. A clothing insulation value of $CLO = 0.5$ and an activity level of $MET = 1.0$ were assumed, in accordance with [40]. The software automatically adjusts the clothing of occupants within a range of ± 0.25 CLO, depending on internal environmental conditions. Lighting was assumed to consist of LED bulbs with a power consumption of 3 W and luminous efficacy of 90 lm/W each (total of 81 W). The number of bulbs in each zone was determined based on the size and intended use of the room. Lighting schedules were aligned with individual room occupancy patterns. Electrical appliances, such as laptops, televisions, and household electronics, were included, and their power consumption was set for each zone based on the intended use and manufacturer data (total of 5.3 kW). For each room, an equipment usage schedule was set according to the time occupants spent in the building and used each device: in bedrooms, laptops (3×40 W) were assumed to be in use from 16:00 to 23:00 daily; in a bathroom, a washing machine (1450 W) operated three hours a week; in a living room and kitchen, a television (175 W) operated from 18:00 to 21:00 daily, a coffee machine (200 W)—one hour per day, a microwave (500 W)—two hours per week, a dishwasher (1450 W)—three hours per week, an oven (1450 W)—three hours per week.

Domestic hot water consumption was set at 80 litres per person per day [41], and its usage was scheduled. The total losses in the HVAC system were assumed to be 0.2 W/m² of floor area with 50% of the lost heat penetrating into the rooms.

Year-round energy analyses were conducted to select the most energy-efficient ventilation system and thermal and electrical energy sources for the newly designed building, through the optimisation of the non-renewable primary energy index. The analyses were carried out in the following stages:

1. Analysis and selection of the mechanical ventilation system in the building—Constant Air Volume (CAV) or Variable Air Volume (VAV).
2. Analysis and selection of the photovoltaic modules' configuration depending on location and exposure (southern and eastern roof surface and on the ground in the southern direction), which determined the tilt angle and possible maximum area and power of photovoltaic modules.
3. Analysis and selection of solar thermal collectors, considering two types (flat and vacuum) and two orientations (south and east) of collectors.
4. Replacement of the air-source heat pump with a ground-source heat pump.

The first two stages of the research were carried out simultaneously, while the subsequent stages were based on the most energy-efficient solutions from earlier stages.

In the first two stages, six computational variants were defined, which are presented in Table 2. These variants differed in the type of mechanical ventilation system (CAV or VAV) as well as the exposure, location, and power of the photovoltaic installation. Variants 1 and 4 differed in the exposure of the photovoltaic installation, which was oriented to the east, unlike the other variants with southern exposure. Variants 2 and 3, as well as 5 and 6, differed in the size of the photovoltaic installation. In the variants with a freestanding ground-mounted structure, the surface area was larger compared to the rooftop-mounted installation, which was limited by the roof's surface area.

For variants 4–5, with the CAV ventilation system, the supply air volume flow rate was set according to the intended use of each room, as specified in [42]. The total ventilation air volume flow rate for the CAV system was 450 m³/h.

In variants 1–3, the mechanical ventilation system VAV was equipped with an automatic ventilation flow rate control system using CO₂ sensors to adjust the supply air volume flow rate according to the number of occupants in each room. The diffuser efficiency was set to

50% of the required hygienic airflow for a given room when occupants were absent, and 100% of the ventilation airflow when their presence was detected, based on the increased CO₂ levels in the room. A minimum CO₂ concentration of 400 ppm was assumed in the absence of occupants, with a maximum CO₂ concentration of 1000 ppm. The maximum calculated ventilation air volume flow rate for the VAV system was 318 m³/h.

Table 2. Computational variants.

Variant	Ventilation System	PV Modules Surface Area, m ²	Tilt Angle of PV Modules, °	PV Modules Exposure and Location	PV Installation Power, kW _p
1	VAV	70	44	east, roof	6.6
2	VAV	40	55	south, roof	4.3
3	VAV	100	45	south, ground	10.7
4	CAV	70	44	east, roof	6.6
5	CAV	40	55	south, roof	4.3
6	CAV	100	45	south, ground	10.7

The three PV system variants analysed were selected to evaluate the impact of surface area and tilt angle to reflect diverse architectural and spatial conditions, as well as orientation and placement to address practical constraints and optimise energy yield based on location-specific solar irradiance conditions. This approach was deliberately focused on assessing how these parameters affect the annual energy-saving potential and primary energy index of the building. The analysis aimed to establish a foundational understanding of optimal PV module placement within the context of a holistic building energy performance evaluation.

2.3. Methodology for Calculating the Non-Renewable Primary Energy Index Value

For all variants, the calculations of the non-renewable primary energy index value were carried out in accordance with Equations (1)–(6), presented in [43].

$$EP = Q_p / A_f, \quad \text{kWh/m}^2/\text{year} \quad (1)$$

where

Q_p —year-round demand for non-renewable primary energy for technical systems, kWh/year

A_f —an area of rooms with regulated air temperature, m²

$$Q_p = Q_{p,H} + Q_{p,W} + Q_{p,C} + Q_{p,L}, \quad \text{kWh/year} \quad (2)$$

where

$Q_{p,H}$ —year-round demand for non-renewable primary energy for the heating system, kWh/year

$Q_{p,W}$ —year-round demand for non-renewable primary energy for the preparation of domestic hot water, kWh/year

$Q_{p,C}$ —year-round demand for non-renewable primary energy for the cooling system, kWh/year

$Q_{p,L}$ —year-round demand for non-renewable primary energy for the lighting installation, kWh/year

$$Q_{p,H} = Q_{f,H} \cdot w_H + E_{el,aux,H} \cdot w_{el}, \quad \text{kWh/year} \quad (3)$$

$$Q_{p,W} = Q_{f,W} \cdot w_W + E_{el,aux,W} \cdot w_{el}, \quad \text{kWh/year} \quad (4)$$

$$Q_{p,C} = Q_{f,C} \cdot w_C + E_{el,aux,C} \cdot w_{el}, \quad \text{kWh/year} \quad (5)$$

$$Q_{p,L} = Q_{f,L} \cdot w_{el}, \quad \text{kWh/year} \quad (6)$$

where

$Q_{f,H}$ —year-round demand for final energy supplied to the building for the heating system, kWh/year

$Q_{f,W}$ —year-round demand for final energy supplied to the building for preparation of domestic hot water, kWh/year

$Q_{f,C}$ —year-round demand for final energy supplied to the building for the cooling system, kWh/year

$Q_{f,L}$ —year-round demand for final energy supplied to the building for the lighting installation, kWh/year

w_i —non-renewable primary energy input factor for production and delivery of [43]:

energy for the heating system (w_H factor, for solar energy (energy from PV installation) equal 0), -

energy for the preparation of domestic hot water (w_W factor, for solar energy (energy from PV installation) equal 0), -

energy for the cooling system (w_C factor), -

electrical energy (w_{el} factor, for system power grid equal 2.5), -

$E_{el,aux,H}$ —year-round demand for auxiliary final energy supplied to the building for the heating system, kWh/year

$E_{el,aux,W}$ —year-round demand for auxiliary final energy supplied to the building for preparation of domestic hot water, kWh/year

$E_{el,aux,C}$ —year-round demand for auxiliary final energy supplied to the building for the cooling system, kWh/year

The values of year-round demand for final energy and auxiliary energy supplied to the building for the heating system and preparation of domestic hot water were obtained through simulations conducted using the IDA ICE 4.8 software. Based on these results, the value of the non-renewable primary energy index was calculated.

Lighting installation calculations were excluded, as lighting requirements for single-family houses are not addressed in the energy analysis for the EP index, in accordance with [43].

3. Results and Discussion

To select the heating energy source for the designed building, heat gains and losses, as well as the use of thermal energy in the building, were calculated using the IDA ICE 4.8 software. Based on the results of the electrical energy usage calculations, a photovoltaic installation was chosen. Additionally, an analysis of the free energy gain from the photovoltaic system and the air heat recovery unit was conducted for each variant. For each calculation variant, the year-round non-renewable primary energy index values were calculated. Based on these, the most energy-efficient variant was selected. Subsequently, further possibilities for optimising the building's energy performance were analysed.

3.1. Heat Balance of the Designed Building

To better understand the building's energy performance, the analysis of the building's heat balance is essential. This approach helps assess how various factors influence the overall heating and cooling requirements. Figure 6 presents the year-round distribution of heat gains and losses for the analysed building for Variants 1–3 with the VAV ventilation system. The total year-round heat losses in the building amounted to 18,504 kWh, while

the heat gains were 15,335 kWh. The heat balance includes heat losses through the external building envelope and for heating the ventilation supply air, as well as heat gains from electronic devices, lighting, and occupants. The year-round heat losses through the external walls and thermal bridges were 13,139 kWh. The heat losses for heating the supply air were 5352 kWh. Additionally, the balance accounted for heat losses in the HVAC system, which amounted to 14 kWh. Heat gains from electronic devices were 2919 kWh, from lighting 139 kWh, and from occupants 1954 kWh. Heat gains due to air infiltration were also considered, amounting to 12 kWh. The heat balance also includes heat losses and gains through windows due to radiation and penetration through the window frame. During the winter period (November–January), heat losses through the windows were 400 kWh, while during the summer and transitional periods (February–October), heat gains through the windows were 10,688 kWh.

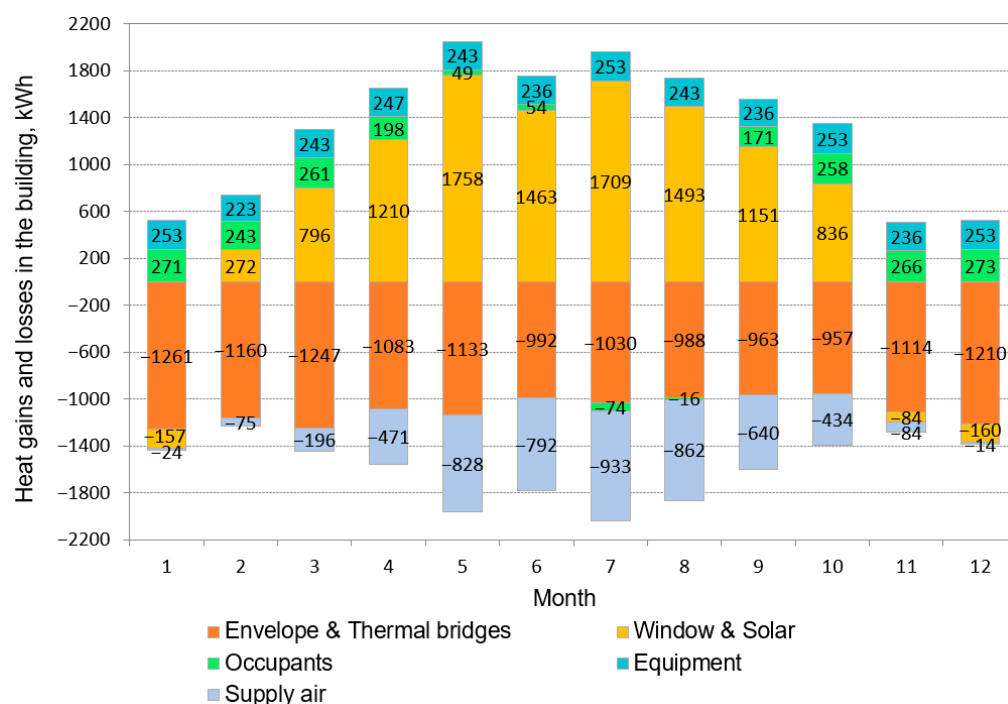


Figure 6. Year-round heat gains and losses in the building for Variants 1–3.

For Variants 4–6 with the CAV ventilation system, the heat losses for heating the supply air were 33% higher compared to Variants 1–3, amounting to 7130 kWh.

The obtained results highlight the advantages of the energy-efficient design of the building. Due to the significant glazing of the building's envelope, particularly the southern external wall, especially in the living room and kitchen area, as well as the external walls in the nighttime part of the building, where floor-to-ceiling windows were installed, the heat gains from solar radiation were maximised, accounting for 70% of the total heat gains. As a result, total heat gains balanced 83% of the building's year-round heat losses. Furthermore, the well-insulated building envelope contributed to stabilising the monthly heat losses throughout the year, preventing an increase in heat losses during the winter period. At the same time, the increase in the building's thermal insulation increases the risk of overheating during the summer period, which is mitigated by higher energy consumption for mechanical ventilation, aimed at maintaining the set indoor air temperature.

IDA ICE heat losses, presented in Figure 6, are calculated dynamically based on detailed models of building components and systems. Heat loss through building envelopes depends on the U-values of materials, surface areas, and the temperature difference between indoor and outdoor environments. Thermal bridges are accounted for using linear and

point thermal transmittance coefficients. For windows, both glazing and frame properties, as well as edge effects, are considered. Ventilation heat losses are determined by airflow rates, temperature differences, and air properties, with adjustments for heat recovery if a system is installed. These calculations adapt to hourly variations in weather and system conditions, providing a comprehensive analysis of heat loss.

3.2. Thermal Energy Consumption in the Building

To further evaluate the energy performance of the building, it is essential to examine how thermal energy is distributed across different operational needs throughout the year. This analysis helps understand the contributions of various energy-consuming systems to the building's overall performance. Figure 7 shows the year-round distribution of thermal energy consumption in Variants 1–3 for space heating, domestic hot water preparation, and ventilation supply air heating. The total amount of heat delivered to the floor heating system (considering losses associated with heat generation and distribution) amounted to 3274 kWh. The total heat delivered to the heating coil in the HRV unit was 1022 kWh. From May to October, no energy was required for heating. The total heat delivered to the domestic hot water system was 6827 kWh per year, with an average of 569 kWh per month. The distribution of heat used for domestic hot water heating remained constant throughout the year due to the assumptions made regarding hot water usage.

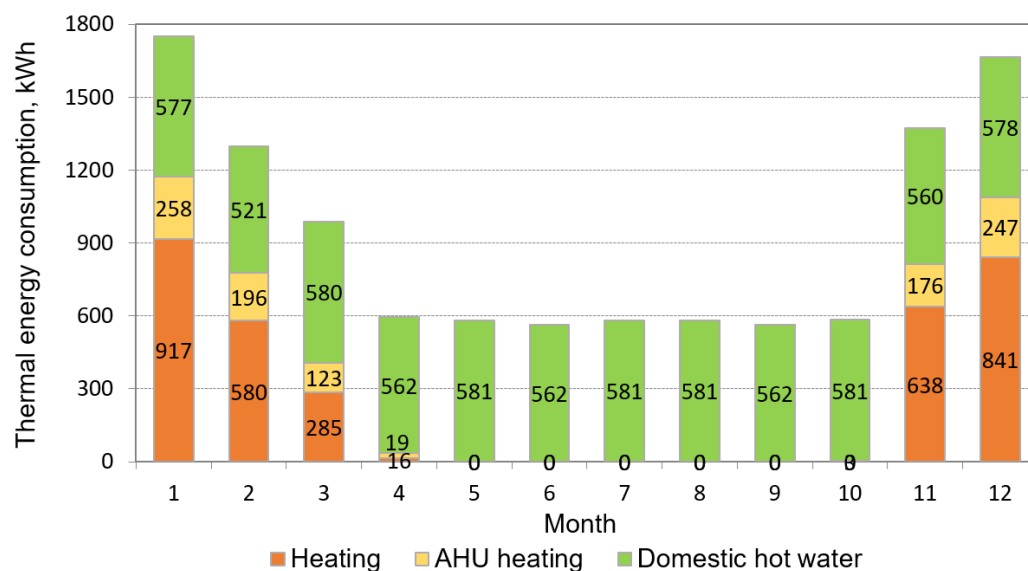


Figure 7. Year-round thermal energy consumption in the analysed building for Variants 1–3.

In Variants 4–6, the heat consumption for heating the supply air was 75% higher than in Variants 1–3, amounting to 1784 kWh.

3.3. Electrical Energy Consumption in the Building

To fully evaluate the energy demand of the building, it is essential to consider the electricity consumption associated with various systems and equipment. This includes energy use for both essential services and auxiliary components. Figure 8 shows the year-round electrical energy consumption for electronic equipment, lighting, heat pump compressor, and auxiliary HVAC system energy (i.e., circulation pumps, fans in the HRV unit) in Variants 1–3. The total energy consumption for electronic equipment was 1954 kWh, for lighting 114 kWh, for the heat pump 2815 kWh, and for auxiliary energy 657 kWh. The total year-round electricity demand for the building was 5540 kWh.

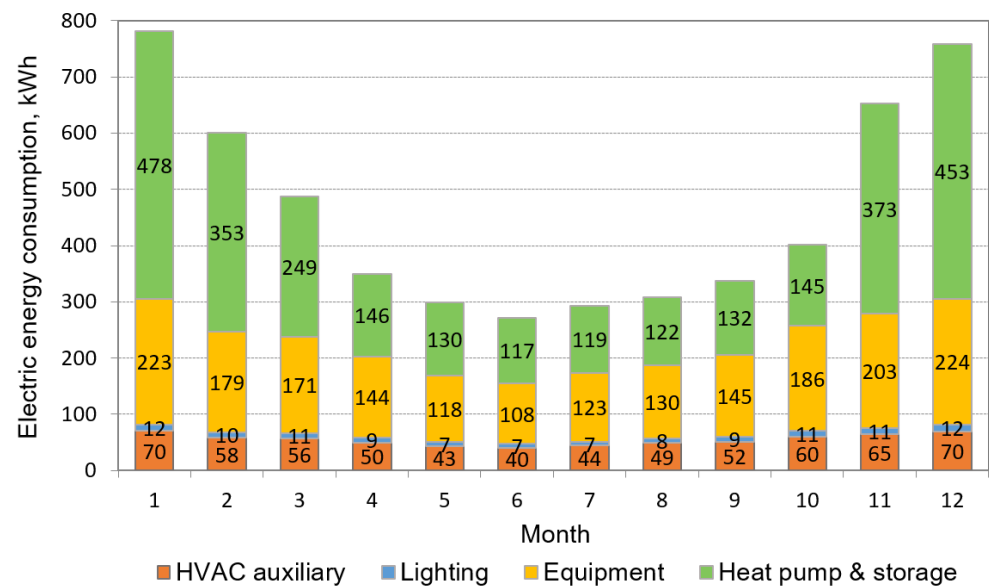


Figure 8. Year-round electrical energy consumption in the analysed building for Variants 1–3.

In Variants 4–6, the auxiliary electrical energy use in the HVAC system was 99% higher, and the energy demand for the heat pump compressor was 9% higher than in Variants 1–3, amounting to 1321 kWh and 3068 kWh, respectively. This was due to the higher ventilation air volume flow rate, which the fan had to handle in the CAV system.

3.4. Generated Free Energy

The performance of the PV system is influenced by factors such as the orientation and location of the PV modules. These factors are integral to determining the overall electrical energy generation efficiency. Figure 9 presents the year-round distribution of the generated electrical energy in the PV system, depending on the orientation and location of the PV modules in the different computational variants. The largest amount of energy, amounting to 10,797 kWh/year, was generated in Variants 3 and 6, in which the PV modules were located on a free-standing structure on the ground and oriented towards the south. The location of the PV modules on the ground, without the limitation of the roof area, allowed for the largest surface area of the PV modules, which was 100 m². In Variants 1 and 4, the PV modules, with a surface area of 70 m², were located on the eastern roof surface, generating 5881 kWh/year, which was 83% lower than in Variants 3 and 6. In Variants 2 and 5, the PV modules, with a surface area of 40 m², were located on the southern roof surface, generating 4247 kWh/year, which was 154% lower than in Variants 3 and 6. Analysing the monthly distribution, it can be observed that there is a sharp decrease in the amount of energy generated during the winter months. For example, in Variant 1, in December, the energy generated was more than seven times lower than in May. This is primarily due to the significant shortening of the day, meaning less time for the PV modules to be exposed to sunlight, and the lowest position of the sun above the horizon during this period.

The efficiency of heat recovery in ventilation systems significantly contributes to reducing the overall energy consumption in the building. The process of heat recovery from ventilated air is essential for optimising energy use, particularly in buildings with mechanical ventilation systems. Table 3 presents the year-round distribution of recovered energy in the building through the heat recovery process of ventilated air. This value depended on the ventilation air volume flow rates in the VAV and CAV systems in the respective variants. In Variants 4–6, equipped with the CAV system, 63% more energy was recovered compared to Variants 1–3 with the VAV system. This difference resulted from a 42% higher ventilation air volume flow rate in the CAV system variants compared to the

maximum value in the VAV system variants. In the summer, the ground heat exchanger was utilised to cool the ventilation supply air, ensuring thermal comfort in the building without the use of air conditioning.

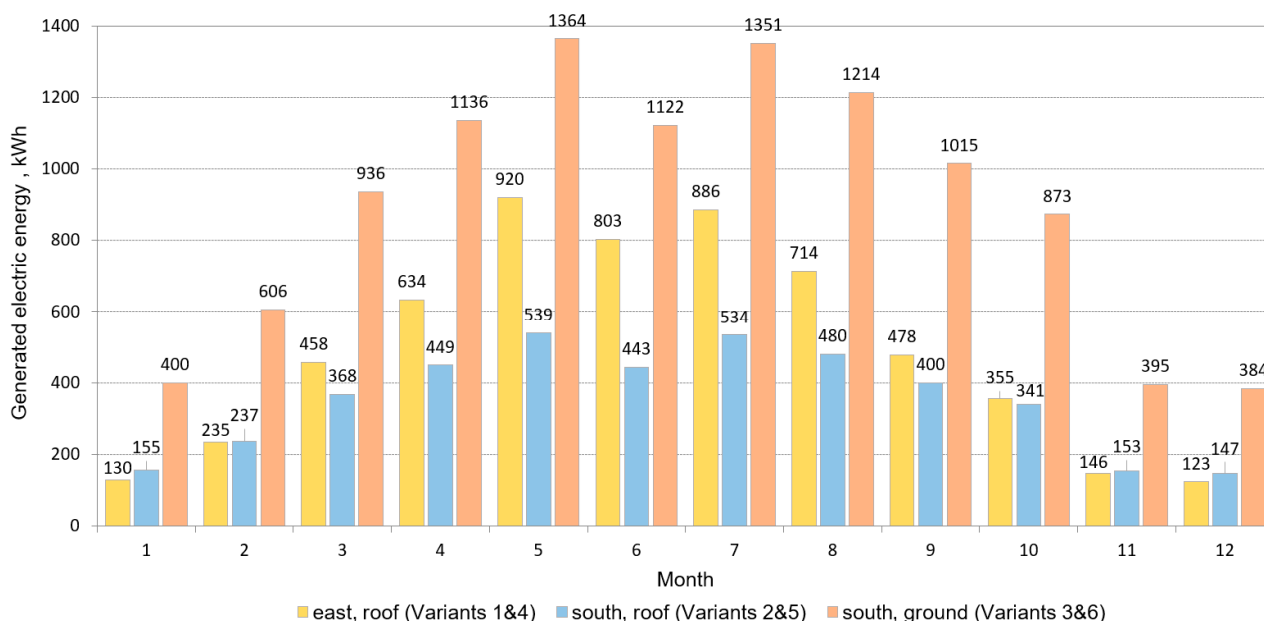


Figure 9. Year-round generated electrical energy depending on the orientation and location of the PV modules.

Table 3. Recovered free energy in the building through the heat recovery process of ventilated air.

Month	VAV (Variants 1–3), kWh	CAV (Variants 4–6), kWh
1	1263	2062
2	1160	1882
3	1232	2003
4	817	1323
5	496	809
6	350	576
7	259	425
8	276	453
9	550	893
10	764	1215
11	1154	1873
12	1248	2043
Total	9568	15,558

3.5. Analysis of the Non-Renawable Primary Energy Index

The analysis of the non-renewable primary energy (EP) index value is essential for evaluating the environmental impact of a building’s energy consumption. This index reflects the amount of non-renewable energy needed to operate the building’s systems and provides a benchmark for comparing different energy strategies.

Table 4 presents the following for each computational variant:

- The values of electrical energy demand for powering the building’s technical systems, i.e., lighting, heating, and domestic hot water system (operation of the heat pump compressor) as well as auxiliary energy for the HVAC system (operation of HRV fans and circulation pumps).

- The amount of electrical energy supplied to the technical systems by the photovoltaic installation (assuming a self-consumption rate of 40%) and the amount of electrical energy supplied by the power grid.
- The values of the year-round non-renewable primary energy index value.

Table 4. Primary energy index values for Variants 1–6.

Variant	Lighting, kWh/Year	Technical System HVAC Aux, kWh/Year	Heat Pump, kWh/Year	Energy from the PV Installation, kWh/Year	Energy from the System Power Grid, kWh/Year	Primary Energy Index, kWh/m ² /Year
1	114	657	2815	2352	1234	16
2	114	657	2815	1699	1887	25
3	114	657	2815	4319	0	0
4	114	1321	3068	2352	2151	28
5	114	1321	3068	1699	2804	37
6	114	1321	3068	4319	0	0

Variants 1 and 2, equipped with the VAV ventilation system, exhibited lower primary energy index values (16 kWh/m²/year and 25 kWh/m²/year, respectively) compared to the corresponding Variants 4 and 5 with the CAV system (28 kWh/m²/year and 37 kWh/m²/year, respectively). This difference was attributed to higher electricity consumption for the powering and auxiliary energy of the HVAC system in the CAV variants, caused by the larger volume flow rate of the ventilation air. Variants 3 and 6 demonstrated the lowest primary energy index value, equal to 0 kWh/m²/year. This was due to the largest photovoltaic module surface area installed on a ground-mounted structure. The absence of space constraints, as opposed to roof-mounted systems in other variants, allowed for the highest electricity production in these cases. All computational variants met the criterion of the maximum value of the non-renewable primary energy index for single-family buildings, which must not exceed 70 kWh/m²/year [18].

Based on the results of the analyses conducted, it was determined that the most advantageous solution in terms of the EP index value for the designed building is the application of the VAV ventilation system. Regarding the photovoltaic installation on the roof, a south-facing orientation is the most favourable. In the analysed building, the unit value of electricity generated by the PV installation mounted on the south-facing roof surface was 42 kWh/m²/year, compared to 34 kWh/m²/year for the east-facing roof surface. However, due to the east-facing roof surface being 30 m² larger, allowing for more PV modules to be installed, mounting the modules on the east-facing surface is the more advantageous solution for this building. The most favourable option for PV installation among all variants is its placement on the ground. With a PV module area of 100 m², the building required no electricity from the grid, thus achieving a zero-energy building status. However, this option demands a significant plot area, potentially limiting its feasibility for many single-family homes, especially considering the space required for a horizontal ground heat exchanger installation. Additionally, such a solution may increase investment costs due to factors such as the need for foundation construction, while the modules themselves may be more susceptible to damage. For these reasons, it was decided to examine how the EP index value could be reduced in Variants 1 and 2 with the VAV ventilation system, in which PV modules were mounted on the roof, to achieve a building performance as close as possible to that of a zero-energy building—one of the criteria of the 4E Idea.

3.6. Optimisation of the Non-Renewable Primary Energy Index

To further enhance the building's energy performance, two variants of solar thermal collector installations—flat-plate and vacuum—were analysed. They were mounted on the southern and eastern roof surfaces, depending on the location of the PV modules in Variants

1 and 2. Subsequently, for the selected solar thermal installation variant characterised by the highest energy efficiency, an analysis of the use of a ground-source heat pump instead of an air-source heat pump was conducted.

The selection of solar thermal collectors was carried out using the T*SOL 2023 software [44] based on the year-round demand for domestic hot water calculated in the IDA ICE 4.8 software. The following calculation variants were established as a result of this selection:

- Variant 1.1: HVAC and PV installation from Variant 1 + two flat-plate solar thermal collectors mounted on the southern roof surface. Parameters of a single thermal collector: aperture area of 2.33 m², efficiency of 78%, linear heat loss coefficient of 4.14 W/m²·K, and square heat loss coefficient of 0.0145 W/m²·K.
- Variant 1.2: HVAC and PV installation from Variant 1 + two vacuum solar thermal collectors mounted on the southern roof surface. Parameters of a single thermal collector: aperture area of 1.6 m², efficiency of 77%, linear heat loss coefficient of 1.256 W/m²·K, and square heat loss coefficient of 0.005 W/m²·K.
- Variant 2.1: HVAC and PV installation from Variant 2 + two flat-plate solar thermal collectors mounted on the eastern roof surface, with parameters as in Variant 1.1.
- Variant 2.2: HVAC and PV installation from Variant 2 + two vacuum solar thermal collectors mounted on the eastern roof surface, with parameters as in Variant 1.2.

Flat-plate and vacuum solar thermal collectors were selected to reflect the two widely used collector technologies, which differ in efficiency and suitability under varying climatic conditions. The location of PV modules and solar thermal collectors was varied to assess the influence of orientation and roof geometry on energy yield. This accounts for real-world scenarios where building constraints or aesthetic considerations might dictate the placement of these systems.

Figure 10 shows the arrangement of solar thermal collectors and PV modules in Variants 1.1, 1.2, 2.1, and 2.2.

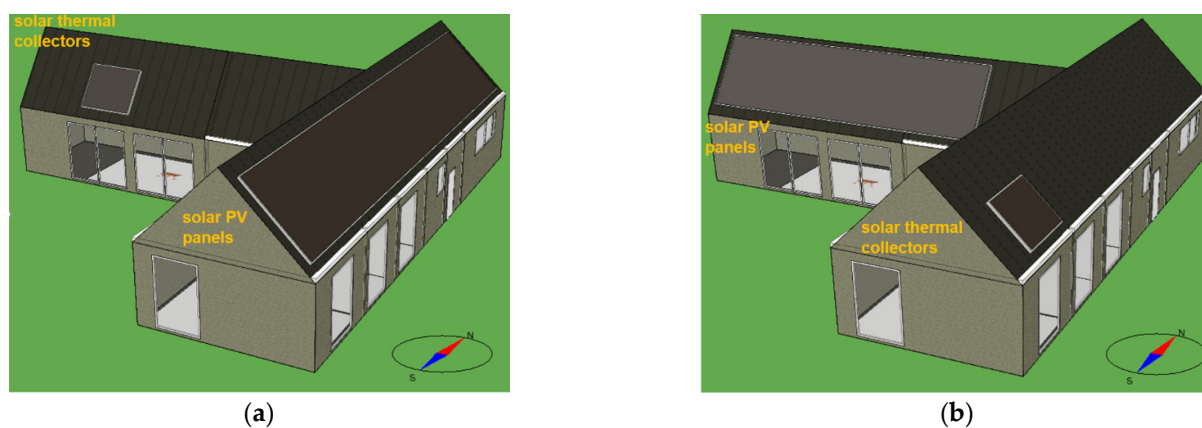


Figure 10. The arrangement of solar thermal collectors and photovoltaic panels in Variants: (a) 1.1 and 1.2, (b) 2.1 and 2.2.

To assess the performance of the solar thermal collectors, the amount of solar radiation energy absorbed is an important factor. These data allow for a comparison of the energy contributions from solar thermal systems across different design variants. Figure 11 presents the amount of solar radiation energy absorbed by the solar thermal collectors in Variants 1.1–2.2. Over a year, the highest amount of solar energy was absorbed by vacuum tube solar thermal collectors oriented southwards (Variant 1.2), amounting to 2908 kWh/year. The second-highest value was absorbed by vacuum tube solar thermal collectors oriented eastwards (Variant 2.2) at 2090 kWh/year. Flat-plate solar thermal collectors exhibited lower levels of absorbed solar energy. For flat-plate collectors oriented southwards (Variant 1.1), the absorbed energy was

1668 kWh/year, while those oriented eastwards (Variant 2.1) absorbed 1077 kWh/year. Thus, it can be concluded that vacuum tube solar thermal collectors with southern exposure were more efficient in terms of absorbed solar energy.

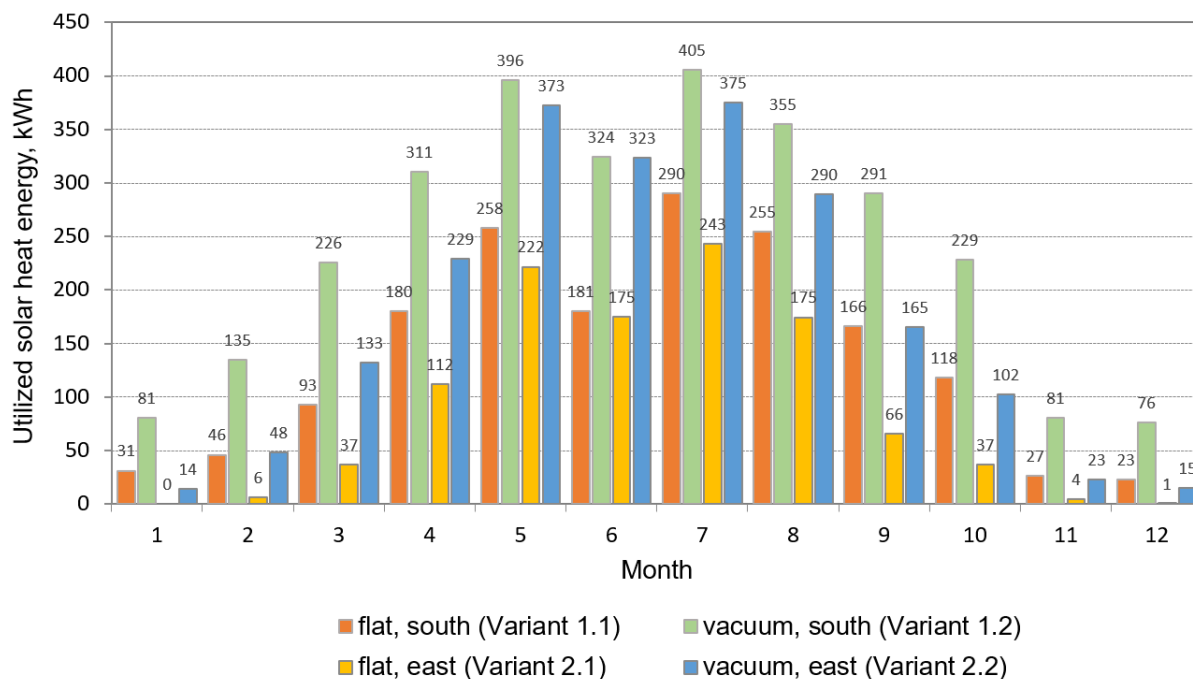


Figure 11. Solar radiation energy absorbed by solar thermal collectors in Variants 1.1–2.2.

Analysing the year-round distribution of solar energy gained by the solar thermal collectors reveals that vacuum tube solar collectors were particularly more effective than flat-plate solar collectors during winter months when the angle of solar radiation is the lowest. For instance, in January, the solar energy yield of the vacuum tube solar system in Variant 1.2 was 161% higher than that of the flat-plate solar system in Variant 1.1. During the summer, this difference decreased but remained significant; for example, in July, the yield of vacuum tube solar collectors (Variant 1.2) was 40% higher compared to flat-plate solar collectors (Variant 1.1).

The distribution of power consumption by the heat pump compressor is a crucial aspect in evaluating the overall energy efficiency of the building. The comparison between variants with and without solar thermal collectors highlights the impact of renewable energy integration on the system's performance. Figure 12 shows the heat pump compressor power distribution in Variant 1, without solar thermal collectors, and Variants 1.1 and 1.2, equipped with flat-plate and vacuum-tube solar thermal collectors, respectively. It can be observed that the greatest reduction in the operational load of the heat pump compressor due to the solar thermal installation occurred between early May and late September. This resulted from the fact that during this period the system worked mainly for domestic hot water preparation. For part of this period, on days with high solar energy gains, the heat pump did not need to operate at all. Vacuum-tube solar collectors contributed to a greater reduction in heat pump operation compared to flat-plate solar collectors. During the remaining part of the year, when the heat pump also operated for heating purposes, the reduction in compressor load due to the solar thermal installation was minimal. However, it is notable that even during the winter months, solar collectors occasionally reduced the workload of the heat pump compressor, depending on the prevailing weather conditions. The figure also highlights that the selected heat pump was equipped with an inverter compressor. This type of compressor operates by adapting its power and speed to varying conditions and individual user needs.

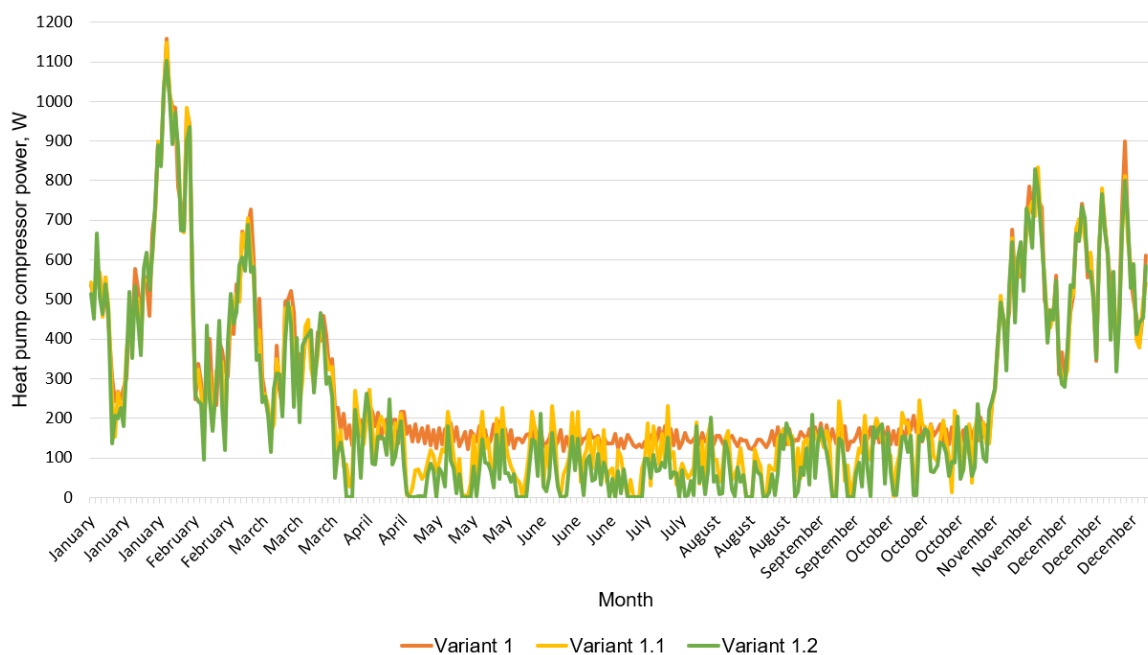


Figure 12. Year-round distribution of heat pump compressor power in Variants 1.1–1.2.

The integration of renewable energy systems, such as solar thermal collectors, can significantly affect the performance and efficiency of heating installations. Combining various technologies, such as heat pumps and solar systems, can considerably reduce overall energy consumption. Table 5 presents the impact of retrofitting the heat pump installation with a solar thermal system. The installation of solar collectors on the southern roof surface resulted in a reduction in energy consumption by the heat pump by 497 kWh/year for flat-plate solar collectors (Variant 1.1) and 680 kWh/year for vacuum solar collectors (Variant 1.2). In the case of solar collectors installed on the eastern roof surface, the energy consumption by the heat pump was reduced by 233 kWh/year for flat-plate solar collectors (Variant 2.1) and by 399 kWh/year for vacuum solar collectors (Variant 2.2). Thus, the installation of south-facing solar collectors resulted in a greater reduction in the heat pump compressor power, by 113% for flat-plate solar collectors and 70% for vacuum solar collectors, compared to the east-facing variants. At the same time, energy consumption by auxiliary devices increased due to the addition of a circulation pump. The most advantageous variants in terms of optimising the primary energy index were the installation of south-facing vacuum and flat-plate solar collectors, with EP index values of 8 kWh/m²/year (Variant 1.2) and 10 kWh/m²/year (Variant 1.1), respectively. Retrofitting Variant 2 with solar collectors resulted in a smaller reduction in the EP value compared to the variant without solar collectors than in the case of retrofitting Variant 1. Therefore, although Variant 2 exhibited a higher EP index value, the most favourable variant from this group, Variant 2.2, was characterised by an EP index value that was higher by 12 kWh/m²/year than the corresponding Variant 1.2.

In the final stage of the analysis of the possibility of optimising the EP index value for the analysed building, an analysis was carried out regarding the use of a ground-source heat pump instead of an air-source heat pump. A ground-source heat pump with a heating capacity of 6 kW and a COP of 5.5 was selected. The thermal efficiency of the ground was assumed to be 20 W/m², in accordance with the guidelines [45], which recommend adopting this value when the parameters of the ground are unknown. It was assumed that the horizontal ground heat exchanger would be placed at a depth of 1.5 m. At this depth, the ground temperature is at least 6 °C [45] and, according to it the COP value for the ground-source heat pump, this was determined based on the manufacturer's data. The

surface area of the ground heat exchanger was calculated according to the guidelines [45] and was 241 m². The ground temperature was assumed to be constant throughout the year, set at 8 °C. Propylene glycol was selected as the heat carrier fluid in the ground heat exchanger installation. The energy analysis was carried out based on Variant 1.2, which had the lowest EP index value.

Table 5. The primary energy index values for Variants 1-2.2.

Variant	Lighting, kWh/Year	Technical System HVAC Aux, kWh/Year	Heat Pump, kWh/Year	Energy from the PV Installation, kWh/Year	Energy from the System Power Grid, kWh/Year	Primary Energy Index, kWh/m ² /Year
1	114	657	2815	2352	1234	16
1.1	114	708	2318	2352	788	10
1.2	114	708	2135	2352	605	8
2	114	657	2815	1699	1887	25
2.1	114	708	2582	1699	1705	22
2.2	114	708	2416	1699	1539	20

Table 6 presents the impact of replacing the air-source heat pump (Variant 1.2) with the ground-source heat pump (Variant 7). The energy consumption by the compressor decreased by 458 kWh/year as a result of using a device with a higher COP value and adopting a constant ground temperature, as opposed to a variable outdoor air temperature throughout the year. As a result, the use of the ground-source heat pump led to a reduction in the EP index value by 6 kWh/m²/year compared to the variant with the air-source heat pump. Ultimately, the designed building, with a VAV ventilation system with heat recovery, an on-grid photovoltaic installation, vacuum solar thermal collectors, and a ground-source heat pump, was characterised by an EP index value of 2 kWh/m²/year. If an off-grid photovoltaic system with an energy storage battery had been used in the building, it could be assumed that the designed building would have achieved a zero-energy building characteristic, as the self-consumption of electricity would have been nearly 100%, as opposed to the 40% in the analysed variant.

Table 6. The primary energy index values for Variants 1.2 and 7.

Variant	Lighting, kWh/Year	Technical System HVAC Aux, kWh/Year	Heat Pump, kWh/Year	Energy from the PV Installation, kWh/Year	Energy from the System Power Grid, kWh/Year	Primary Energy Index, kWh/m ² /Year
1.2	114	708	2135	2352	605	8
7	114	740	1645	2352	147	2

4. Conclusions

The paper presents the concept of a newly designed single-family building based on the 4E Idea, which assumes that the building should be energy-efficient, ecological, economical, and incorporate ergonomic design solutions. The energy efficiency criterion stipulates that the building should generate zero energy consumption or a positive year-round energy balance. The aim of the paper was to conduct multi-variant energy simulations of the proposed building, the results of which were intended to enable the selection of an HVAC system and a renewable energy sources concept that would ensure that the building's energy performance is as close as possible to a zero-energy building. It was analysed how the following factors influenced the reduction in the non-renewable primary energy index value: the type of mechanical ventilation system (CAV and VAV); the orientation and power of the photovoltaic installation; the exposure and type of solar thermal collectors (flat-plate and vacuum); and the type of heat pump (air and ground source). Based on the obtained results, the following conclusions were drawn:

- The architectural and structural concept of the building enabled the maximisation of heat gains and the reduction in heat losses through the external building envelope. Due to the significant glazing of the building envelope, the solar heat gains accounted for 70% of the total heat gains. As a result, the total heat gains covered 83% of the building's year-round heat losses. Furthermore, the well-insulated building envelope contributed to stabilising the monthly heat losses throughout the entire year.
- The analysis of the type of supply-and-exhaust mechanical ventilation with heat recovery showed that the VAV system is more energy-efficient than the CAV system. The variant in which an air-source heat pump and a VAV ventilation system were applied exhibited half the energy consumption compared to the corresponding variant with a CAV system (657 kWh/year for the VAV system and 1321 kWh/year for the CAV system). This difference resulted from the reduced ventilation air volume flow rate, as the VAV system adjusted the air supply to the current CO₂ concentration levels in the rooms. Consequently, the heat pump compressor consumed 253 kWh/year less energy, as it was required to supply less heat to warm the ventilation air.
- The analysis of the photovoltaic modules' location showed that a southern exposure is generally the most favourable for solar installations. The specific energy yield of the PV modules installed on the southern roof surface was 42 kWh/m²/year, compared to 34 kWh/m²/year for the eastern roof surface. However, due to the eastern roof's 30 m² larger surface area, which allowed for the installation of more PV modules, installing the modules on this surface proved to be the more advantageous solution for the analysed building. The variant featuring a VAV ventilation system, an air-source heat pump, and PV modules installed on the eastern roof surface (with a total module area of 70 m² and a capacity of 6.6 kWp) was characterised by an EP index value of 16 kWh/m²/year. In contrast, the southern roof surface installation (with a total module area of 40 m² and a capacity of 4.3 kWp) had an EP index value of 25 kWh/m²/year. In the case of the variant in which the PV modules were installed on a ground-mounted structure with a southern orientation and a surface area of 100 m², the building achieved zero energy characteristics. However, this solution requires a significant plot area, involves higher investment costs, and presents a greater risk of damage, making it less suitable for widespread implementation.
- The analysis of the location and type of solar thermal collectors showed that the most favourable variant for optimising the PE index value was the installation of vacuum tube solar collectors on the southern roof surface. This configuration resulted in an EP index value of 8 kWh/m²/year, and thus a two-fold reduction in the EP index value compared to the variant without solar thermal collectors. The installation of solar thermal collectors alleviated the workload of the heat pump compressor for domestic hot water preparation and contributed to a reduction in the heat pump compressor's electricity consumption by 629 kWh/year. This shows that under variable climatic conditions, vacuum tube solar thermal collectors exhibit higher efficiency compared to flat-plate solar thermal collectors.
- The analysis of the type of heat pump used indicated that the variant incorporating a ground-source heat pump with a horizontal ground heat exchanger demonstrated superior efficiency. This variant was characterised by a four-fold reduction in the EP index value compared to the variant with an air-source heat pump. This resulted from the higher COP value of the ground-source heat pump, which was constant throughout the year due to the stable ground temperature, in contrast to the fluctuating temperature of atmospheric air. Additionally, the installation of solar thermal collectors contributed to reducing the heat pump's workload and improving ground regeneration, particularly during the summer months.

- For the analysed building equipped with a VAV mechanical ventilation system with heat recovery, an on-grid photovoltaic installation, vacuum solar thermal collectors, and a ground-source heat pump with a horizontal heat exchanger, a primary energy index value of 2 kWh/m²/year was achieved. The self-consumption of the generated electrical energy in the building was assumed to be 40%. It can be expected that implementing an off-grid photovoltaic system could result in achieving a zero-energy building characteristic.

The study has several limitations that should be noted. The simulations were conducted for a specific single-story building with particular construction characteristics, which may limit the generalizability of the results. Fixed parameters for occupant behaviour, such as device usage schedules and comfort temperatures, were assumed, which do not fully reflect variability in real-world scenarios. Additionally, local climatic conditions were used, which may not account for future climate changes, such as shorter periods of low temperatures. The analysis also excluded economic factors due to the dynamic nature of energy prices and equipment costs, which are influenced by social and political factors. Despite these limitations, the findings provide a valuable starting point for further research and analysis. As a result of the conducted analysis, a concept for an energy-efficient building was developed, which, in terms of architectural and construction design, as well as the configuration of the HVAC system and renewable energy sources installation, can serve as a starting point for future energy-efficient single-family building designs. Further research should be carried out for the variant incorporating electric energy storage to achieve further optimisation of the PE index value.

Author Contributions: Conceptualization, P.C., J.K. and D.W.-J.; methodology, P.C. and J.K.; software, P.C.; formal analysis, P.C. and J.K.; writing—original draft preparation, P.C.; writing—review and editing, J.K. and P.C.; visualisation, D.W.-J. All authors have read and agreed to the published version of the manuscript.

Funding: This research received no external funding.

Data Availability Statement: The original contributions presented in the study are included in the article, further inquiries can be directed to the corresponding author.

Acknowledgments: The work is supported by the Polish Ministry of Education and Science within the research subsidy.

Conflicts of Interest: The authors declare no conflicts of interest.

References

1. van Staalduinen, W.; Dantas, C.; Ferenczi, A.; Klimczuk, A.; Freitas, A.; Abreu Cordeiro, B.; Guley Goren Soares, B.; Pineda Revilla, B.; Hilario, C.; Vassiliou, C.; et al. White Paper: Designing the Perfect New European Bauhaus Neighbourhood. 2024. Available online: <https://open.icm.edu.pl/items/0501e238-886e-40b0-81eb-c259afd03fc1> (accessed on 1 December 2024).
2. GUS Budownictwo w 1 Kwartale 2024 Roku. Available online: <https://stat.gov.pl/obszary-tematyczne/przemysl-budownictwo-srodki-trwale/budownictwo/budownictwo-w-1-kwartale-2024-roku,13,22.html> (accessed on 13 November 2024).
3. EU Energy Statistical Pocketbook and Country Datasheets. Available online: https://energy.ec.europa.eu/data-and-analysis/eu-energy-statistical-pocketbook-and-country-datasheets_en (accessed on 18 November 2024).
4. GUS Energy Consumption in Households in 2021. Available online: <https://stat.gov.pl/en/topics/environment-energy/energy/energy-consumption-in-households-in-2021,2,6.html> (accessed on 1 December 2024).
5. GUS Energy Efficiency in Years 2012–2022. Available online: <https://stat.gov.pl/en/topics/environment-energy/energy/energy-efficiency-in-years-20122022,5,21.html> (accessed on 1 December 2024).
6. Greenhouse Gas Emissions from Energy Use in Buildings in Europe. Available online: <https://www.eea.europa.eu/en/analysis/indicators/greenhouse-gas-emissions-from-energy> (accessed on 1 December 2024).
7. Kania, G.; Kwiecień, K.; Malinowski, M.; Gliniak, M. Analyses of the Life Cycles and Social Costs of CO₂ Emissions of Single-Family Residential Buildings: A Case Study in Poland. *Sustainability* **2021**, *13*, 6164. [[CrossRef](#)]

8. Poland—Countries & Regions. Available online: <https://www.iea.org/countries/poland/energy-mix> (accessed on 18 November 2024).
9. Zator, S.; Skomudek, W. Impact of DSM on Energy Management in a Single-Family House with a Heat Pump and Photovoltaic Installation. *Energies* **2020**, *13*, 5476. [[CrossRef](#)]
10. Niekurzak, M.; Lewicki, W.; Drożdż, W.; Miązek, P. Measures for Assessing the Effectiveness of Investments for Electricity and Heat Generation from the Hybrid Cooperation of a Photovoltaic Installation with a Heat Pump on the Example of a Household. *Energies* **2022**, *15*, 6089. [[CrossRef](#)]
11. Hesaraki, A.; Madani, H. *Energy Performance of Ground-Source Heat Pump and Photovoltaic/Thermal (PV/T) in Retrofitted and New Buildings: Two Case Studies Using Simulation and On-Site Measurements*; SINTEF Academic Press: Cambridge, MA, USA, 2020; ISBN 978-82-536-1679-7.
12. Kemmler, T.; Thomas, B. Design of Heat-Pump Systems for Single- and Multi-Family Houses Using a Heuristic Scheduling for the Optimization of PV Self-Consumption. *Energies* **2020**, *13*, 1118. [[CrossRef](#)]
13. Pater, S. Increasing Energy Self-Consumption in Residential Photovoltaic Systems with Heat Pumps in Poland. *Energies* **2023**, *16*, 4003. [[CrossRef](#)]
14. Baraskar, S.; Günther, D.; Wapler, J.; Lämmle, M. Analysis of the Performance and Operation of a Photovoltaic-Battery Heat Pump System Based on Field Measurement Data. *Sol. Energy Adv.* **2024**, *4*, 100047. [[CrossRef](#)]
15. Thorsteinsson, S.; Kalae, A.A.S.; Vogler-Finck, P.; Stærmoose, H.L.; Katic, I.; Bendtsen, J.D. Long-Term Experimental Study of Price Responsive Predictive Control in a Real Occupied Single-Family House with Heat Pump. *Appl. Energy* **2023**, *347*, 121398. [[CrossRef](#)]
16. Nalini Ramakrishna, S.K.; Björner Brauer, H.; Thiringer, T.; Håkansson, M. Social and Technical Potential of Single Family Houses in Increasing the Resilience of the Power Grid during Severe Disturbances. *Energy Convers. Manag.* **2024**, *321*, 119077. [[CrossRef](#)]
17. Drozd, W.; Kowalik, M. Analysis of Renewable Energy Use in Single-Family Housing. *Open Eng.* **2019**, *9*, 269–281. [[CrossRef](#)]
18. Obwieszczenie Ministra Rozwoju i Technologii z Dnia 15 Kwietnia 2022 r. w Sprawie Ogłoszenia Jednolitego Tekstu Rozporządzenia Ministra Infrastruktury w Sprawie Warunków Technicznych, Jakim Powinny Odpowiadać Budynki i Ich Usytuowanie. Available online: <https://isap.sejm.gov.pl/isap.nsf/DocDetails.xsp?id=WDU20220001225> (accessed on 10 December 2024).
19. Nielsen, T.R.; Drivsholm, C. Energy Efficient Demand Controlled Ventilation in Single Family Houses. *Energy Build.* **2010**, *42*, 1995–1998. [[CrossRef](#)]
20. Lu, D.B.; Warsinger, D.M. Energy Savings of Retrofitting Residential Buildings with Variable Air Volume Systems across Different Climates. *J. Build. Eng.* **2020**, *30*, 101223. [[CrossRef](#)]
21. Bai, H.Y.; Liu, P.; Justo Alonso, M.; Mathisen, H.M. A Review of Heat Recovery Technologies and Their Frost Control for Residential Building Ventilation in Cold Climate Regions. *Renew. Sustain. Energy Rev.* **2022**, *162*, 112417. [[CrossRef](#)]
22. Cavazzini, G.; Zanetti, G.; Benato, A. Analysis of a Domestic Air Heat Pump Integrated with an Air-Geothermal Heat Exchanger in Real Operating Conditions: The Case Study of a Single-Family Building. *Energy Build.* **2024**, *315*, 114302. [[CrossRef](#)]
23. Halios, C.H.; Landeg-Cox, C.; Lowther, S.D.; Middleton, A.; Marczylo, T.; Dimitroulopoulou, S. Chemicals in European Residences—Part I: A Review of Emissions, Concentrations and Health Effects of Volatile Organic Compounds (VOCs). *Sci. Total Environ.* **2022**, *839*, 156201. [[CrossRef](#)]
24. Poirier, B.; Guyot, G.; Geoffroy, H.; Woloszyn, M.; Ondarts, M.; Gonze, E. Pollutants Emission Scenarios for Residential Ventilation Performance Assessment. A Review. *J. Build. Eng.* **2021**, *42*, 102488. [[CrossRef](#)]
25. Khoshnav, S.M.; Rostami, R.; Mohamad Zin, R.; Štreimikienė, D.; Mardani, A.; Ismail, M. The Role of Green Building Materials in Reducing Environmental and Human Health Impacts. *Int. J. Environ. Res. Public Health* **2020**, *17*, 2589. [[CrossRef](#)] [[PubMed](#)]
26. Lim, A.-Y.; Yoon, M.; Kim, E.-H.; Kim, H.-A.; Lee, M.J.; Cheong, H.-K. Effects of Mechanical Ventilation on Indoor Air Quality and Occupant Health Status in Energy-Efficient Homes: A Longitudinal Field Study. *Sci. Total Environ.* **2021**, *785*, 147324. [[CrossRef](#)]
27. Winnicka-Jasłowska, D.; Jastrzębska, M.; Kaczmarczyk, J.; Łażniewska-Piekarczyk, B.; Skóra, P.; Kobiątko, B.; Kołodziej, A.; Mól, B.; Lasyk, E.; Brzęczek, K.; et al. Projekt koncepcyjny domu mieszkalnego opartego na Idei 4E. Project-based learning realizowany w Politechnice Śląskiej. *Builder* **2023**, *307*, 12–19. [[CrossRef](#)]
28. Pan, Y.; Zhu, M.; Lv, Y.; Yang, Y.; Liang, Y.; Yin, R.; Yang, Y.; Jia, X.; Wang, X.; Zeng, F.; et al. Building Energy Simulation and Its Application for Building Performance Optimization: A Review of Methods, Tools, and Case Studies. *Adv. Appl. Energy* **2023**, *10*, 100135. [[CrossRef](#)]
29. Tihana, J.; Ali, H.; Apse, J.; Jekabsons, J.; Ivancovs, D.; Gaujena, B.; Dedov, A. Hybrid Heat Pump Performance Evaluation in Different Operation Modes for Single-Family House. *Energies* **2023**, *16*, 7018. [[CrossRef](#)]
30. Xue, T.; Jokisalo, J.; Kosonen, R. Cost-Effective Control of Hybrid Ground Source Heat Pump (GSHP) System Coupled with District Heating. *Buildings* **2024**, *14*, 1724. [[CrossRef](#)]
31. Sankelo, P.; Ahmed, K.; Mikola, A.; Kurnitski, J. Renovation Results of Finnish Single-Family Renovation Subsidies: Oil Boiler Replacement with Heat Pumps. *Energies* **2022**, *15*, 7620. [[CrossRef](#)]

32. Mazzeo, D.; Romagnoni, P.; Matera, N.; Oliveti, G.; Cornaro, C.; De Santoli, L. Accuracy of the Most Popular Building Performance Simulation Tools: Experimental Comparison for a Conventional and a PCM-Based Test Box. In Proceedings of the Building Simulation 2019—16th IBPSA International Conference and Exhibition, Rome, Italy, 2–4 September 2019; pp. 4530–4537.
33. Mazzeo, D.; Matera, N.; Cornaro, C.; Oliveti, G.; Romagnoni, P.; De Santoli, L. EnergyPlus, IDA ICE and TRNSYS Predictive Simulation Accuracy for Building Thermal Behaviour Evaluation by Using an Experimental Campaign in Solar Test Boxes with and without a PCM Module. *Energy Build.* **2020**, *212*, 109812. [[CrossRef](#)]
34. Schaffer, M.; Bugenings, L.A.; Larsen, O.K. Validating a Building Performance Simulation Model of a Naturally Ventilated Double Skin Facade. *J. Phys. Conf. Ser.* **2023**, *2654*, 012092. [[CrossRef](#)]
35. EN 12831-1:2017; Energy Performance of Buildings. Method for Calculation of the Design Heat Load Space Heating Load, Module M3-3. European Committee for Standardization: Brussels, Belgium, 2017.
36. Allouhi, A. Solar PV Integration in Commercial Buildings for Self-Consumption Based on Life-Cycle Economic/Environmental Multi-Objective Optimization. *J. Clean. Prod.* **2020**, *270*, 122375. [[CrossRef](#)]
37. Analysis of Self-Consumption of Energy from Grid-Connected Photovoltaic System for Various Load Scenarios with Short-Term Buffering | Discover Applied Sciences. Available online: <https://link.springer.com/article/10.1007/s42452-019-0432-5> (accessed on 15 November 2024).
38. IDA ICE—Simulation Software | EQUA. Available online: <https://www.equa.se/en/ida-ice> (accessed on 9 December 2024).
39. American Society of Heating, Refrigerating and Air Conditioning Engineers. *ASHRAE Handbook; Fundamentals* (SI Edition); American Society of Heating, Refrigerating and Air Conditioning Engineers: Atlanta, GA, USA, 2013.
40. *ASHRAE 55:2010; Thermal Environmental Conditions for Human Occupancy*. ASHRAE: Atlanta, GA, USA, 2010.
41. Rozporządzenie Ministra Infrastruktury z Dnia 14 Stycznia 2002 r. w Sprawie Określenia Przeciętnych Norm Zużycia Wody (Dz.U. 2002 Nr 8 Poz. 70). Available online: <https://isap.sejm.gov.pl/isap.nsf/DocDetails.xsp?id=WDU20020080070> (accessed on 10 December 2024).
42. PN-83/B-03430/Az3:2000; Wentylacja w Budynkach Mieszkalnych Zamieszkania Zbiorowego i Użyteczności Publicznej—Wymagania. Wydawnictwa Normalizacyjne PKNiM: Warszawa, Poland, 1983.
43. Rozporządzenie Ministra Rozwoju i Technologii z Dnia 28 Marca 2023 r. Zmieniające Rozporządzenie w Sprawie Metodologii Wyznaczania Charakterystyki Energetycznej Budynku Lub Części Budynku Oraz Świadcstw Charakterystyki Energetycznej. (Dz.U. 2023 Poz. 697). Available online: <https://isap.sejm.gov.pl/isap.nsf/DocDetails.xsp?id=WDU20230000697> (accessed on 10 December 2024).
44. T*SOL Online | Free Solar Thermal Calculator. Available online: <https://online.tsol.de/en> (accessed on 9 December 2024).
45. Polska Organizacja Rozwoju Technologii Pomp Ciepła. *Wytyczne Projektowania, Wykonania i Odbioru Instalacji z Pompami Ciepła; Część 1. Dolne Źródła Do Pomp Ciepła; PEMP, Wydanie Drugie*: Kraków, Poland, 2021.

Disclaimer/Publisher’s Note: The statements, opinions and data contained in all publications are solely those of the individual author(s) and contributor(s) and not of MDPI and/or the editor(s). MDPI and/or the editor(s) disclaim responsibility for any injury to people or property resulting from any ideas, methods, instructions or products referred to in the content.